A benchmark city for seismic resilience assessment

Shang Qingxue[1†], Guo Xiaodong[2*], Li Quanwang[3§], Xu Zhen[4§], Xie Linlin[5‡], Liu Chaofeng[6§], Li Jichao[1‡] and Wang Tao[1*]

1. *Key Laboratory of Earthquake Engineering and Engineering Vibration, Institute of Engineering Mechanics, China Earthquake Administration, Harbin 150080, China*

2. *Earthquake Resistance and Disaster Mitigation Institute, Beijing University of Technology, Beijing 100022, China*

3. *Department of Civil Engineering, Tsinghua University, Beijing 100084, China*

4. *Beijing Key Laboratory of Urban Underground Space Engineering, School of Civil and Resource Engineering, University of Science and Technology Beijing, Beijing 100083, China*

5. *School of Civil and Transportation Engineering, Beijing University of Civil Engineering and Architecture, Beijing 100044, China*

6. *School of Civil Engineering and Transportation, Hebei University of Technology, Tianjin 300401, China*

Abstract: The concept of seismic resilience has received significant attention from academia and industry during the last two decades. Different frameworks have been proposed for seismic resilience assessment of engineering systems at different scales (e.g., buildings, bridges, communities, and cities). Testbeds including Centerville virtual community (CVC), Memphis testbed (MTB), and the virtual city of Turin, Italy (VC-TI) have been developed during the last decade. However, the resilience assessment results of Chinese cities still require calibration based on a unified evaluation model. Therefore, a geographic information system (GIS)-based benchmark model of a medium-sized city located in the southeastern coastal region of China was developed. The benchmark city can be used to compare existing assessment frameworks and calibrate the assessment results. The demographics, site conditions, and potential hazard exposure of the benchmark city, as well as land use and building inventory are described in this paper. Data of lifeline systems are provided, including power, transportation, water, drainage, and natural gas distribution networks, as well as the locations of hospitals, emergency shelters, and schools. Data from past earthquakes and the literature were obtained to develop seismic fragility models, consequence models, and recovery models, which can be used as basic data or calibration data in the resilience assessment process. To demonstrate the completeness of the data included in the benchmark city, a case study on the accessibility of emergency rescue after earthquakes was conducted, and the preliminary results were discussed. The ultimate goal of this benchmark city is to provide a platform for calibrating resilience assessment results and to facilitate the development of resilient cities in China.

Keywords: seismic resilience; resilience assessment; benchmark model; lifeline systems; fragility models

1 Introduction

Seismic resilience, which is defined as the ability of an engineering system (e.g., buildings, bridges, communities, and cities) to resist, recover from, and adapt to an earthquake (Bruneau *et al.*, 2003) has

attracted significant attention from academia and industry recently. The recovery capacity of a system is quantified as the variation of the functionality over time. The abilities of the system to maintain functionality after earthquakes and to recover from the earthquakes are two crucial properties that a system should possess before or after the occurrence of earthquakes (Yodo and Wang, 2016). The concept of seismic resilience provides a new means of thinking about how to survive and recover from earthquakes.

An assessment of the seismic resilience of a complicated engineering system provides an understanding of the impact of earthquakes in terms of functionality degeneration (robustness), substitutable components (redundancy), recovery time and speed (rapidity), and the available resources (resourcefulness) of the system (Bruneau *et al.*, 2003). The assessment results can help decision-makers to formulate effective strategies in all phases of the earthquakes (Cimellaro *et*

al., 2010). Different frameworks for seismic resilience assessment of engineering systems have been proposed during the last two decades, and qualitative and quantitative methods have been used. Bruneau *et al*. (2003) developed a conceptual assessment framework and a system diagram to improve system resilience by system assessment and modification during the pre- and post-earthquake periods. Chang and Shinozuka (2004) proposed a quantification framework that relates the expected losses in future earthquakes to a community's seismic performance. Miles and Chang (2006) presented a comprehensive conceptual model of functionality recovery that compares the disparity between systems with different levels of disaster preparedness and mitigation decisions. Hu *et al*. (2012) proposed a conceptual evolutionary framework for aseismic decision support for hospitals to integrate a range of engineering and sociotechnical models. Bruneau and Reinhorn (2007) used the percentage of the healthy population, the patient/day treatment capacity, and the repair cost to quantify time-variant resilience.

The Multidisciplinary Center for Earthquake Engineering Research (MCEER) has identified the key steps for quantifying the technical and organizational aspects of resilience. The uncertainties related to the intensity measures, response parameters, performance threshold, performance measures, losses, and recovery time are part of the MCEER framework (Cimellaro *et al*., 2009). Uncertainties induced by these factors should be carefully considered in resilience assessment. And a large number of studies has been conducted to include uncertainties in resilience assessment, for instance, the MCEER framework (Cimellaro *et al*., 2009), probability-based methods (Dong and Frangopol, 2016; Li *et al*., 2019), and probabilistic resilience assessment frameworks (Burton *et al*., 2017; Shang *et al*., 2020).

The MCEER framework was subsequently adopted by Cimellaro *et al*. (2011) to estimate the resilience of hospital systems using a meta-model. The interaction between the technical and organizational aspects was considered by using penalty factors. Cimellaro *et al*. (2010) proposed a framework that integrates direct and indirect losses and a model for the recovery of organizational efficiency to quantify the resilience of hospitals. Cimellaro *et al*. (2016) developed the PEOPLES framework for measuring resilience at different scales (e.g., individual building, city, region, and state); seven different dimensions of resilience were used in a layered approach.

The San Francisco Bay Area Planning and Urban Research Association (SPUR) developed a framework for improving San Francisco's resilience through seismic mitigation policies. The expected seismic performance of buildings and lifeline systems during and after earthquakes are defined in the SPUR framework (SPUR, 2008). The National Institute of Standards and Technology (NIST) developed the Community Resilience Planning Guide for Buildings and Infrastructure Systems (Guide) to help communities enhance resilience by incorporating short- and long-term measures and consider community social goals and their dependencies on the built environment and infrastructure systems (NIST, 2016). The SYNER-G project proposed an integrated general framework for vulnerability assessment of the physical and socio-economic impact and losses of an earthquake and applied this framework to cities including Thessaloniki, L'Aquila, and Vienna (Kyriazis, 2013; Pitilakis*et al*., 2014).

At the national level, the Hyogo Framework for Action (HFA) (UNISDR, 2007; Djalante *et al*., 2012) was created by the United Nations International Strategy for Disaster Reduction (UNISDR) to enable systematic planning, implementation, and evaluation of disaster risk reduction activities to ensure the resilience of nations and communities. The Sendai Framework for Disaster Risk Reduction (SFDRR) (UNISDR, 2015; Kelman and Glantz, 2015) was established based on the HFA to achieve a substantial reduction in disaster risk and losses over the next 15 years. Since 2018, FEMA has been working to develop a new pre-disaster hazard mitigation program, the Building Resilient Infrastructure and Communities (BRIC) program, to improve disaster preparedness, mitigation, response, and recovery programs and outcomes (FEMA, 2020). More and more attention has been paid to resilience assessment and resilient society.

In the aforementioned frameworks, the scale of the target systems ranges from individual buildings and interconnected networks to the community and city levels. However, the resilience assessment results of different frameworks require calibration based on a benchmark model to ensure that the method is valid and can be used by decision-makers. One example of an existing benchmark model is the Centerville Virtual Community (CVC) developed by Ellingwood *et al*. (2016), which is a city of approximately 50,000. At the city level, the Mid-America Earthquake (MAE) Center developed the Memphis Testbed (MTB) to study seismic effects on the city of Memphis (Steelman and Hajjar 2008). Similarly, Noori *et al*. (2017) developed a virtual city (VC-TI) based on the buildings in the city of Turin, Italy. The virtual city covers an area of 120.1 km^2, with a population of 850,000. The above-mentioned models can be used for seismic resilience assessment and calibration. However, the size of the CVC is relatively small. The VC-TI and MTB are representations of typical European and American cities that differ substantially from Chinese cities. Therefore, a benchmark city based on a medium-sized city located in southeastern region of China is developed in this study. Nearly authentic data is provided, and the benchmark model can be used to calibrate resilience assessment frameworks, evaluate the effects of different strategies for resilience improvement and facilitate the construction of seismic resilient city in China. The data format and hierarchy structure can also be extended to other benchmark cities around the world.

The benchmark model is based on Geographic Information System (GIS) models and can be used for secondary development. The benchmark city consists of a residential zone, business zone, industrial park, government agencies, schools, hospitals, and physical lifeline systems. The demographics, site conditions, and potential hazards of the benchmark city model are described in this paper. Detailed information on the building inventory and different lifeline systems is also provided. Data from past earthquakes and the literature were used to develop fragility models, consequence models, and recovery models that can be utilized in the resilience assessment process. A case study on the accessibility of emergency rescue after earthquakes was conducted to demonstrate the completeness of the data included in the benchmark city. The ultimate goal is to provide a platform for calibrating resilience assessment results and to help decision-makers to formulate effective strategies in all phases of earthquakes, i.e., the planning for and the recovery from disasters.

2 Description of the benchmark city

2.1 Demographics

The benchmark model represents a medium-sized city in the southeastern coastal region of China. A summary of the demographics of the benchmark city is presented in Table 1. The total area of the benchmark city is 344.56 km². The urbanization level is typically represented by the proportion of the urban population to the total population and is 60% for this city. The Engel coefficient of urban residents is 33%, and the Gini coefficient is 0.3. The average number of years of education is 14 years, indicating that most of the citizens are high school graduates (12 years) or have a college diploma (≥16 years). The unemployment rate of the urban residents is 2.10%.

2.2 Earthquake hazard

The design earthquake intensity is VII, and the peak ground acceleration (PGA) corresponds to a design-basis earthquake (DBE) is 0.10 g with the exceedance probability of 10% in 50 years. The characteristic period T_g of the site of the entire benchmark city is 0.40 s, according to GB 18306-2015 (2015). The design earthquake group for this benchmark city is categorized as the second group in the Chinese code (GB 50011-2010, 2010). Existing ground-motion models for Chinese cities, such as that provided by Hong and Chao (2019), can be used to map the seismic hazard of this benchmark city.

2.3 Land use of residential areas

The residential area consists of 5 city zones and 14 residential areas, as shown in Fig. 1. The number of citizens in the 14 residential areas is shown in Fig. 1. The residential areas are composed of 337 residential units. The business district covers the center, western, southern, and northern parts of the city. The government center and central business district (CBD) are located in the southern part of the city. Educational areas are scattered all over the city. The northwestern part of the residential area (North district) is an industrial area. The population of the benchmark city is about 690,000. The 346 residential units are shown in Fig. 2.

2.4 Building inventory

The buildings in the benchmark city have several construction types, as shown in Fig. 3(a). There are 9773 buildings in the benchmark city, including 946 unreinforced masonry structures, 3778 reinforced concrete (RC) frame structures, 1621 RC frame shear wall structures, 3420 reinforced masonry structures, and 8 steel frame structures. The proportions of the different structural types are shown in Fig. 3(c). The vast majority of buildings are low-rise buildings (three stories or less, 38.45%) and multi-story buildings (four stories to six stories, 36.75%). These buildings were constructed in different years and were thus designed following different design codes. However, most of the buildings were built after 1989, accounting for 89.56% of the

Table 1 Population demographics of the benchmark city

Indicator	Value
Total area (km²)	344.56
GDP per capita ($)	16218
Urbanization level	60%
Disposable income of urban residents ($)	11141
Per capita net income of rural residents ($)	6346
Engel coefficient of urban residents	33%
Gini coefficient	0.3
Average number of years of education (year)	14
Unemployment rate of urban residents	2.10%

total. During the past three decades, the seismic design codes in China have changed three times, namely GBJ 11-89 (1989), GB 50011-2001 (2001), and GB 50011-2010 (2010). The proportions of buildings constructed in different years are shown in Fig. 3(b). The total occupied area of these buildings is 5.558 km^2, and the total building area covering all building floors is 34.966 km^2. The proportions of occupied areas and building areas of different types of buildings are shown in Figs. 3(d) and 3(e). All the unreinforced masonry structures were built before 1989, and 81.8% are one-story buildings. The statistics of the building height and the building numbers
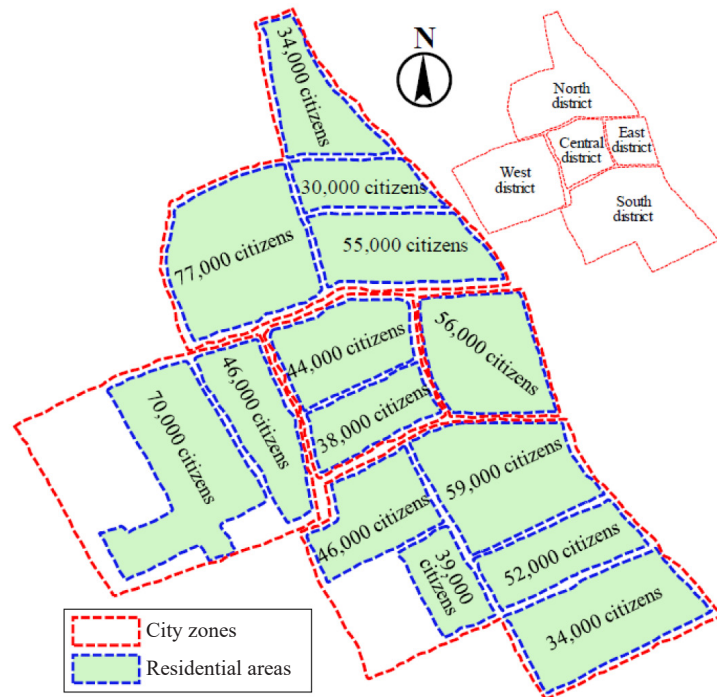

Fig. 1   Five city zones and 14 residential areas of the benchmark city

Fig. 2   Distribution of residential units

are provided in Figs. 3(f)–3(h). It is worth noting that there are 8 super high-rise buildings in this city, and their heights (100 m–256 m) are not listed in Fig. 3(h).

3 Lifeline systems of the benchmark city

Interdependent systems, including individual buildings and lifeline systems in a city, constitute a complex network system. Interdependencies between these systems often exacerbate the initial damage, leading to cascading failures during earthquakes and causing problems for emergency rescues after earthquakes. However, most currently available frameworks or methods focus primarily on one system and do not address the importance of assessing interdependencies (Reiner and McElvaney, 2017). For instance, building damage will result in injuries and death after a huge earthquake. The delivery of emergency rescue instructions relies on the communication system, while its operationality depends on the power distribution network. Damage to transportation systems will influence the speed of delivering injured people to hospitals. Medical treatments in hospitals need electricity to ensure normal operation of medical equipment. Based on the building inventory information in Section 2 and detailed information of lifeline systems in this section, the interdependencies can be considered in seismic resilience assessments. Lifeline systems of the developed benchmark city are designed based on Chinese codes and city planning documents (PAR, 2017). Basic information on the lifeline systems, including the transportation system, the power, water, drainage, and natural gas networks, as well as hospitals, emergency shelters, and schools will be discussed later. Resilience assessments of individual systems or of the entire city and its interconnected and interdependent lifeline systems are feasible using this benchmark model.
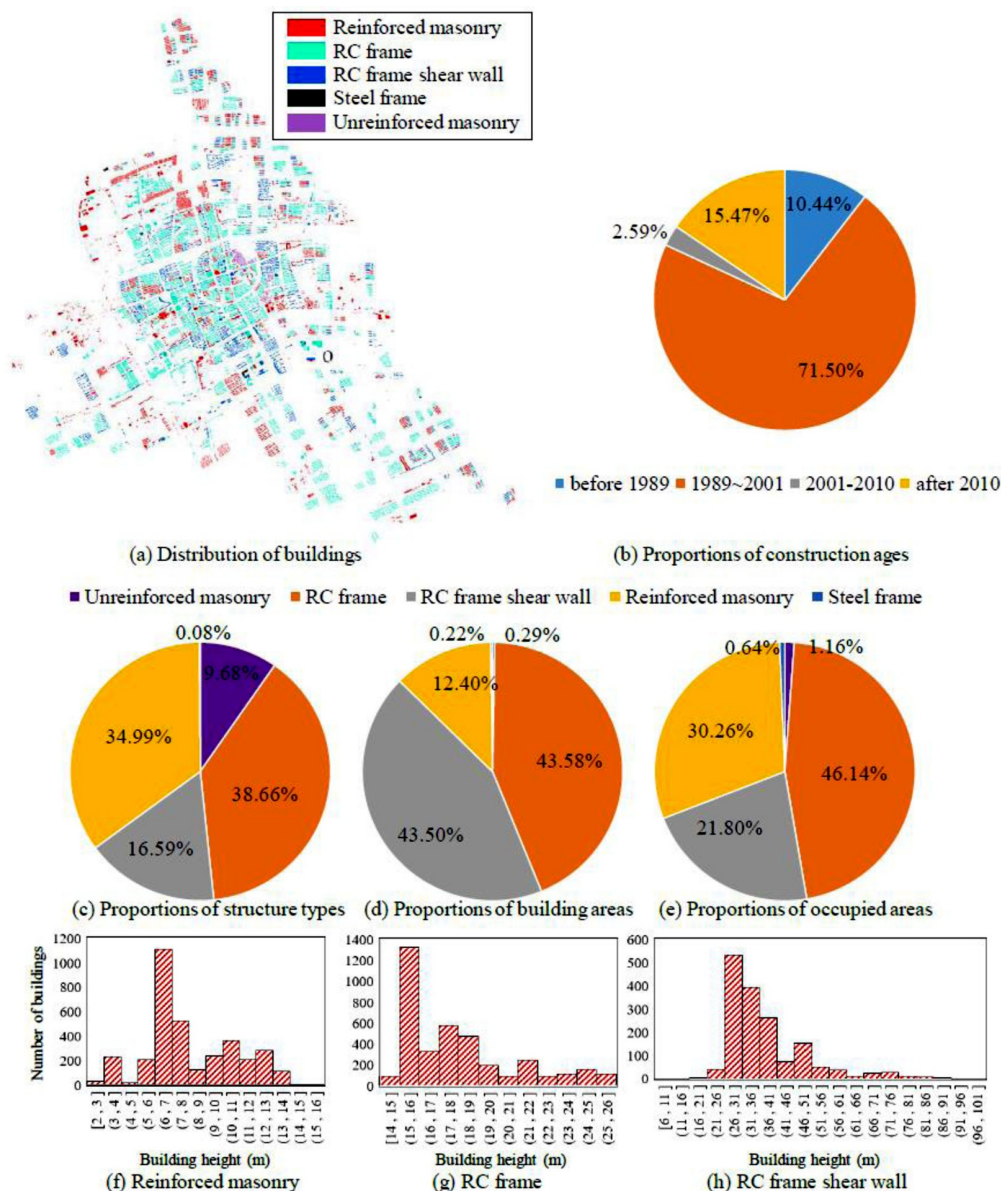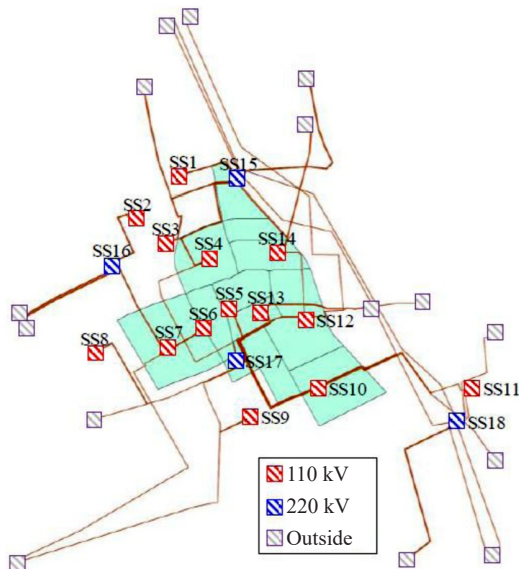

Fig. 3 Building inventory information

3.1 Power distribution network

The power distribution network is shown in Fig. 4. It includes fourteen 110 kV substations, four 220 kV substations, and the distribution lines. The substations are used for the power supply of the benchmark city or to connect to the power grid of other cities or regions. It is worth noting that "outside" represents substations located outside the benchmark city; these are not considered in the model. The capacity of the power distribution network is listed in Table 2.

3.2 Transportation system

The transportation system of the benchmark city consists of roads of different levels with different travel speeds under normal conditions. High-speed roads, major roads, subsidiary roads, and small branch roads comprise the road system. The transportation system also includes 10 masonry arch bridges and 45 simply-supported girder bridges, as shown in Fig. 5(a). The recommended travel speed ranges from 20 km/h to 70 km/h, as shown in Fig. 5(b). The total number of roads is 1133, with a total length of 485.7 km. The recommended travel speeds of the different road levels are listed in Table 3, and the road widths and total road lengths are listed in Table 4. The transportation network, including road width and density of the road network, are shown in Figs. 5(c) and 5(d).

3.3 Water distribution network

The urban water consumption in the benchmark city is 219,164 m^3/day. The benchmark city is supplied with water by a water plant outside the city (with an output of 600,000 m^3/day). Water to the citizens is supplied by two pressure-boosting stations (PBSs), namely PBS 1 (with an output of 200,000 m^3/day) and PBS 2 (with an output of 50,000 m^3/day). The water plant (WP 1) (Fig. 6) is used as an emergency standby water plant (with an output of 150,000 m^3/day). The water distribution network consists of 323 pipe segments, with a total length of 255 km. The diameter, length, and material of the pipe segments, as well as the water demand of the nodes under normal conditions are provided in the benchmark model. The water distribution network is located in a flood plain; thus, the elevations of the nodes are zero for simplicity.

Fig. 4 Power distribution network

Table 2 Capacity information of the power distribution network

Substation name	Voltage (kV)	Capacity (MVA)	Substation name	Voltage (kV)	Capacity (MVA)
SS1	110	3×80	SS10	110	3×80
SS2	110	3×80	SS11	110	2×80
SS3	110	3×80	SS12	110	3×80
SS4	110	2×80	SS13	110	2×80
SS5	110	2×80	SS14	110	2×80
SS6	110	3×80	SS15	220	3×240
SS7	110	3×80	SS16	220	3×240
SS8	110	3×80	SS17	220	2×240
SS9	110	3×80	SS18	220	3×240

Table 3 Road hierarchy and recommended travel speed

Road hierarchy	Recommended travel speed (km/h)	Road length (m)
High-speed road	70	46684
Arterial road	60	149518
Secondary road	50	252209
Branch road	20	37263

(a) Road and bridge distribution

(b) Recommened travel speed (unit: km/h)

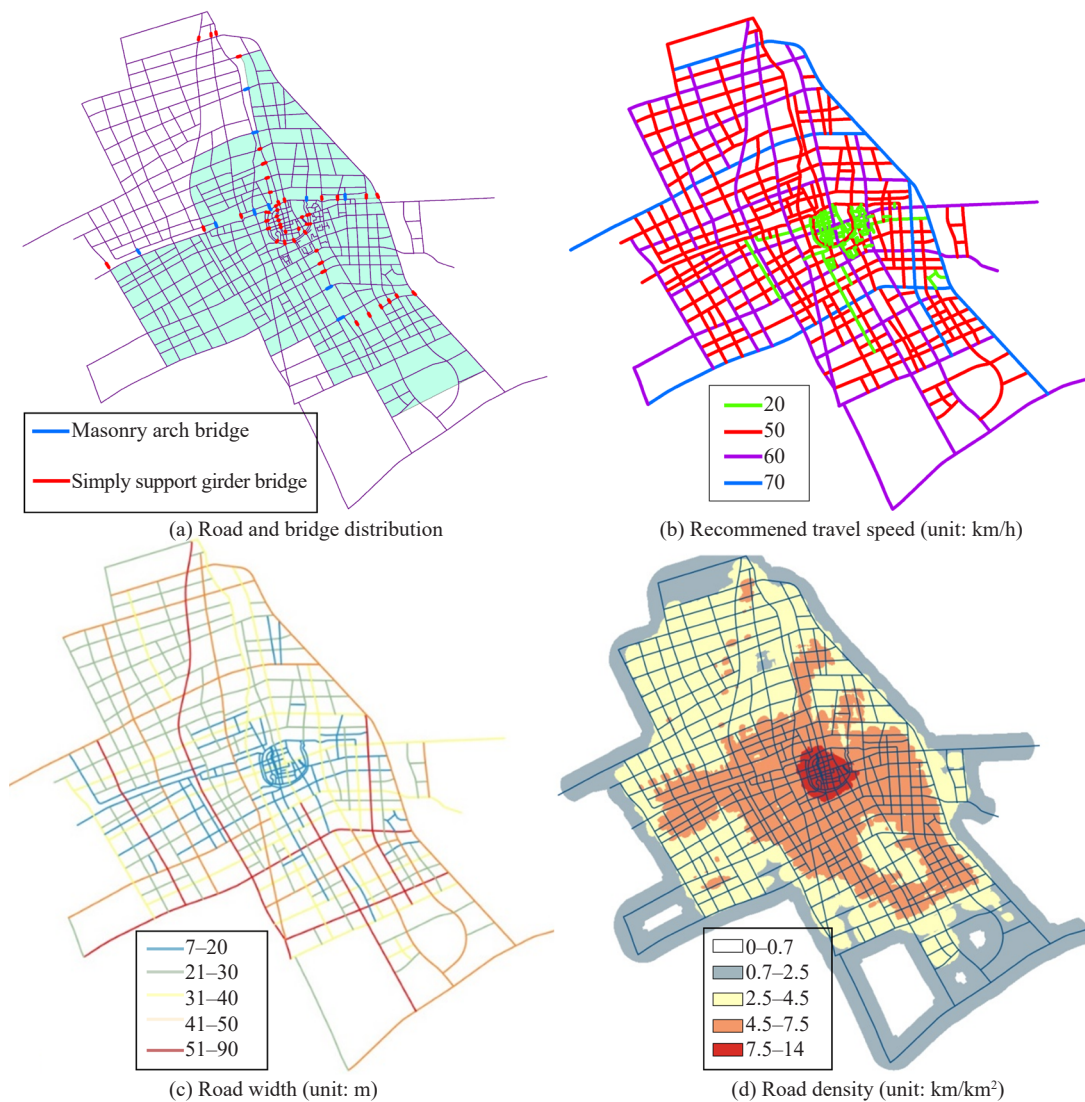(c) Road width (unit: m)

(d) Road density (unit: km/km²)

Fig. 5 Transportation system

3.4 Drainage network

The volume of the centralized sewage treatment plant in the benchmark city is about 163,000 m³/day. The sewage treatment volumes of the four sewage plants (SPs), namely SP 1, SP2, SP3, and SP4 are 20,000 m³/day, 80,000 m³/day, 30,000 m³/day, and 80,000 m³/day, respectively. The sewage treatment volumes of the 18 pump stations are listed in Table 6. The drainage network is shown in Fig. 7. The pipe diameter and length information of the drainage network are provided in Table 7; the diameters of the drainage pipes range from DN400 to DN1200.

3.5 Natural gas distribution network

The natural gas distribution network serves the residential units. The total gas consumption is about 970 million m³/year. As shown in Fig. 8, the gas gate station and regulator stations receive gas from a high-pressure pipe from the supply source outside the city. The gas is sent to the medium-pressure natural gas pipe of each

Table 4 Road width and road length

Road width (m)	Road length (m)
7–20	93075
21–30	159665
31–40	94174
41–50	89297
51–90	49464

residential area after filtration, metering, and pressure adjustment. The liquid natural gas (LNG) supply station is used as a peak regulator gas source or emergency standby gas source. The pipe diameter and length information of the natural gas distribution network are listed in Table 8.

3.6 Hospitals, emergency shelters, and schools

There are eight hospitals in the benchmark city, including four Level 2 hospitals and four Level 3

Table 5   Details of the pipes used in the water distribution network

Diameter (mm)	Material	Number	Total Length (m)	Material	Number	Total Length (m)
200	Cast iron	7	6340	PVC	0	0
300	Cast iron	60	39285	PVC	25	22506
400	Cast iron	33	26337	PVC	57	51265
500	Cast iron	8	6476	PVC	14	11783
600	Cast iron	62	45814	PVC	23	22015
800	Cast iron	11	8545	PVC	0	0
1000	Cast iron	22	13703	PVC	1	605
Sum	-	323	254674			

Table 6   Sewage treatment volumes of pump stations

Pump station name	Volume (10^3 m³/day)	Pump station name	Volume (10^3 m³/day)
JX1	10	J1	6
JX2	25	J2	20
JX3	40	J3	10
X1	10	J4	20
X2	25	N1	20
X3	40	N2	15
X4	18	N3	20
X5	18	N4	20
X6	60	N5	15

Table 7   Pipe information of the drainage network

Pipe diameter	Pipe length (m)
DN400	27988
DN500	62045
DN600	47069
DN700	1560
DN800	45547
DN900	4361
DN1000	27075
DN1200	1099
Total length	216744

Table 8   Pipe information of the natural gas distribution network

Pipe diameter	Pipe length (m)
DN100	63799
DN150	152298
DN200	46469
DN250	31943
DN300	19099
DN350	5851
DN400	3709
Total length	323169
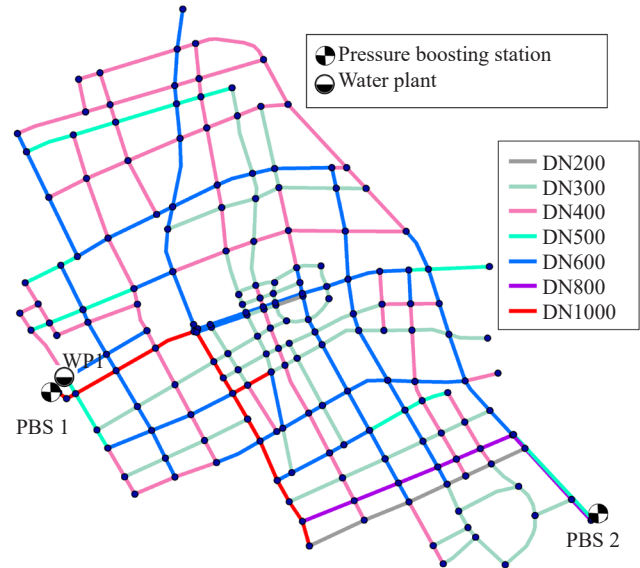
Fig. 6 Water distribution network

hospitals of different sizes (Table 9). The construction types of the hospitals include RC frames and RC frame shear wall structures. A total number of 4,657 patient beds and 4,995 medical staff are available in emergency situations during an earthquake. The numbers of clinical departments and medical laboratories in each hospital are listed in Table 9. The locations of the eight hospitals in the residential units are shown in Fig. 9. In addition to the eight hospitals, there are 20 emergency shelters, which can be used for temporary medical service in case of an emergency. The locations of the educational institutions, including 15 primary schools, eight junior middle schools, and three senior middle schools, are shown in Fig. 9. These schools can also serve as emergency evacuation sites.
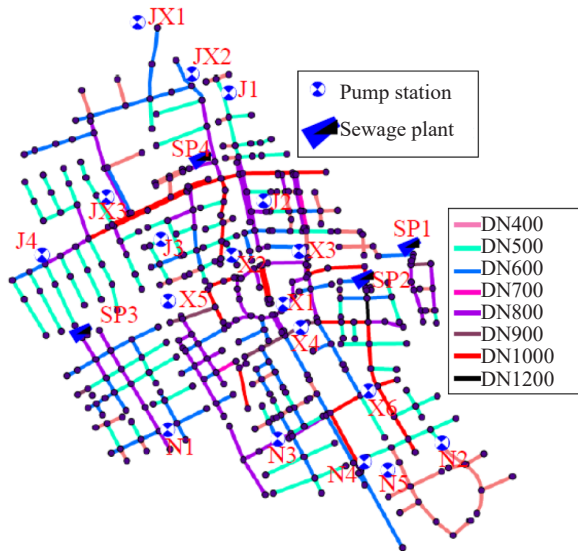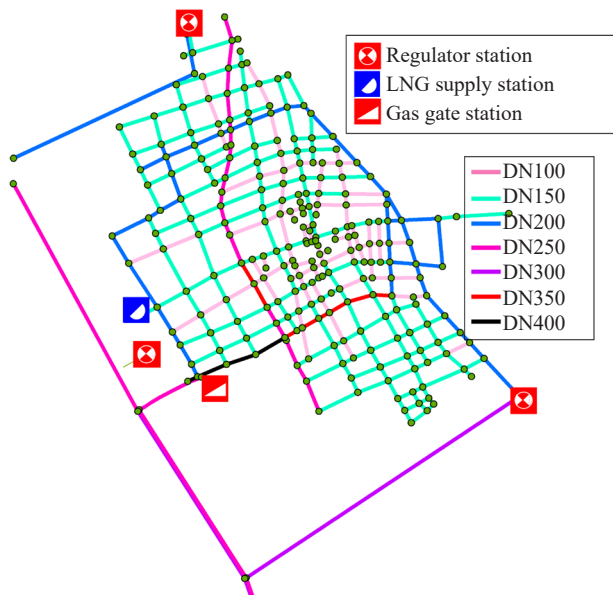
Fig. 7　Drainage network

Fig. 8　Natural gas distribution network

Fig. 9　Hospitals, emergency shelters, and schools

4　Basic models for seismic resilience assessment

4.1　Seismic fragility models

A seismic fragility model is used to define the probability that a component, building, or system exceeds a pre-defined damage state (DS) based on a given engineering demand parameter (*EDP*), e.g., *PGA*, peak floor acceleration (*PFA*), and the maximum inter-story drift ratio (*IDR*). A fragility model is usually idealized as a lognormal distribution function and has been used in seismic resilience assessments to obtain probability-based results. The parameters (including the median values (x_m) and logarithmic standard deviations (β)) used to define the fragility curve with a lognormal distribution have a substantial influence on the assessment results and, therefore, should be carefully selected. Considering that the design codes in China are different from those of other countries, the fragility models provided by the

Table 9　Detailed information on the eight hospitals

Hospital name	Hospital level	Number of stories	Patient beds	Medical staff	Clinical departments	Medical laboratories
H-N-1	Level 2	6	550	600	33	7
H-C-1	Level 3	6	511	654	28	13
H-C-2	Level 3	10	1248	1161	25	7
H-E-1	Level 2	5	150	200	10	4
H-W-1	Level 2	5	80	80	8	3
H-W-2	Level 2	5	218	200	23	7
H-W-3	Level 3	10	900	1000	24	7
H-S-1	Level 3	10	1000	1100	28	8

HAZUS-MH software package (HAZUS-MH MR3, 2003) and FEMA P58 (2012) may be not suitable for seismic performance of buildings and infrastructures in China. Therefore, experimental results, numerical results, and earthquake reconnaissance results from available literatures were collected to develop fragility models which can be used for the proposed benchmark models. Examples of the fragility parameters of different buildings and bridges are listed in Table 10.

The statistical data obtained by Taghavi and Miranda (2003) indicated that non-structural components (NSCs) accounted for most of the investment in a typical building. Although damage to structural components (SCs) is the most important measure of building damage affecting casualties, the damage to NSCs results in the highest economic loss and loss of functionality. Therefore, both SCs and NSCs should be considered in seismic performance or resilience assessments (Filiatrault and Sullivan, 2014). The recent Chinese standard for the seismic resilience assessment of buildings (GB/T 38591-2020, 2020) provides fragility database for NSCs in China and can be used for seismic resilience of the benchmark model. The fragility parameters of the NSCs can also be obtained from the literature on the seismic fragility of NSCs, such as piping systems (Wang et al., 2019), partition walls (Pali et al., 2018), and suspended ceilings (Lu et al., 2018). The fragility curves of drift-sensitive NSCs and acceleration-sensitive NSCs provided by the HAZUS-MH software package (HAZUS-MH MR3, 2003) can also be used as a compromise if fragility parameters of some NSCs are not available.

4.2 Consequence models

A strong correlation is assumed between building damage (both structural and non-structural damage) and the number of casualties and economic loss. The HAZUS-MH software package (HAZUS-MH MR3, 2003) and FEMA P58 (2012) provide consequence models for evaluating the number of casualties and economic losses of buildings. For instance, HAZUS-MH MR3 (2003) defines the four levels of casualty severities as light injuries, hospitalized injuries, life-threatening injuries, and deaths, and it uses event trees to determine the number of casualties caused by an earthquake. FEMA P58 (2012) provides casualty rates for different SCs and NSCs in different damage states. Hingorania et al. (2020) summarized the relevant parameters for predicting potential fatalities and developed consequence models for predicting the loss of life due to the collapse of buildings. However, these data and models may be not suitable for use in Chinese buildings. The Chinese code GB/T 18208.4-2011 (2012) provides models for evaluating direct economic losses caused by earthquakes. GB/T 38591-2020 (2020) states that the number of deaths should be calculated using the product of the personnel density, floor area, and death rate corresponding to each damage state. The number of injuries can be calculated in the same manner, with injury rates corresponding to each damage state. The criteria for determining the damage states of floors and the personnel density of buildings with different functions are provided in GB/T 38591-2020 (2020).

Table 10 Fragility parameters of different buildings and bridges

	EDP	Parameter	Slight damage	Moderate damage	Extensive damage	Complete damage	Reference
Unreinforced masonry	IDR	x_m	0.0008	-	0.002	0.0045	Jiang et al. (2020)
		β	0.35	-	0.30	0.35	
Reinforced masonry	IDR	x_m	0.00063	0.00143	0.00286	0.005	Xiong (2004)
		β	0.35	0.35	0.30	0.35	
RC frame	IDR	x_m	0.00182	0.01	0.02	0.04	Yu et al. (2016)
		β	0.20	0.30	0.30	0.40	
RC frame shear wall	IDR	x_m	0.00125	0.0025	0.005	0.01	Xu (2019)
		β	0.40	0.40	0.40	0.40	
Steel frame	IDR	x_m	0.00333	0.005	0.01	0.01818	Li et al. (2017)
		β	0.40	0.40	0.40	0.40	
Masonry arch bridge	PGA (g)	x_m	0.251	0.475	0.907	2.539	Lin et al. (2017)
		β	1.004	0.887	0.845	0.845	
Simply-supported girder bridge	PGA (g)	x_m	0.237	0.596	1.262	1.286	Lin et al. (2017)
		β	0.998	0.751	0.704	0.357	

The consequence models provided in GB/T 18208.4-2011 (2012) and GB/T 38591-2020 (2020) can be used for seismic resilience assessment of the developed benchmark model.

4.3 Recovery models

FEMA P58 (2012) provides a repair sequence considering parallel repair and series repair for building level recovery. Based on the determined repair schedule, the recovery process of a damaged building can be evaluated in terms of the recovery time and functionality improvement. More detailed repair paths, such as the REDi (Almufti and Willford, 2013) repair sequence and the repair path provided by Shang *et al*. (2020) can also be selected for building recovery assessment. For city-level building recovery, the repair schedule for regional buildings developed by Xiong *et al*. (2020) can be used. However, the recovery process of buildings after earthquakes is highly dependent on the lifeline systems. Therefore, the recovery process of lifeline systems is also a key factor in evaluating the seismic resilience of a city. Kammouh *et al*. (2018) developed recovery models based on statistical data of downtime for different lifeline systems in recent earthquakes. The models are presented in terms of the probability of recovery time. However, the statistical data were collected from different countries worldwide, and the recovery model may not be suitable for Chinese cities. Therefore, in this study, recovery time data of lifeline systems after recent earthquakes in China were analyzed to generate time-based recovery models, as depicted in Fig. 10. The earthquake magnitude (*EM*) was used as the intensity measure since most datasets include this parameter. The recovery model describes the relationship between recovery time of a system after earthquakes and the earthquake magnitude. Data with *EM* ranging from 4.5 to 8.0 were selected to develop the recovery models. It was observed that the recovery time increases slowly when *EM* is small and the increasing trend becomes quite large when *EM* is large. An exponential function (Eq. (1)) was adopted to describe the relationship between recovery time and *EM* considering both the distribution of data and the goodness of fitting. The proposed recovery models can be used to calibrate the evaluation results of different frameworks. It is noteworthy that the data from four past earthquakes in China were used to generate recovery time model for the Gas system. The accuracy shall be noted because of the limited number of samples.

$$T = ae^{bx} \tag{1-1}$$

$$\ln(T) = \ln(a) + bx \tag{1-2}$$

The functionality of a system is improved when the recovery process has been initiated after earthquakes, and the change in functionality over time is usually described using a resilience curve. Figure 11 presents several examples of resilience curves of lifeline systems reported after recent earthquakes (Monsalve and Llera, 2019). For most cases in Fig. 11, the lifeline systems recover quickly after the earthquakes, and the functionality is improved rapidly. After the initial recovery, the rate of recovery decreases. It is observed that the recovery time of lifeline systems internationally is substantially longer than that in China (compared with the predicted data in Fig. 10). This result is attributed to
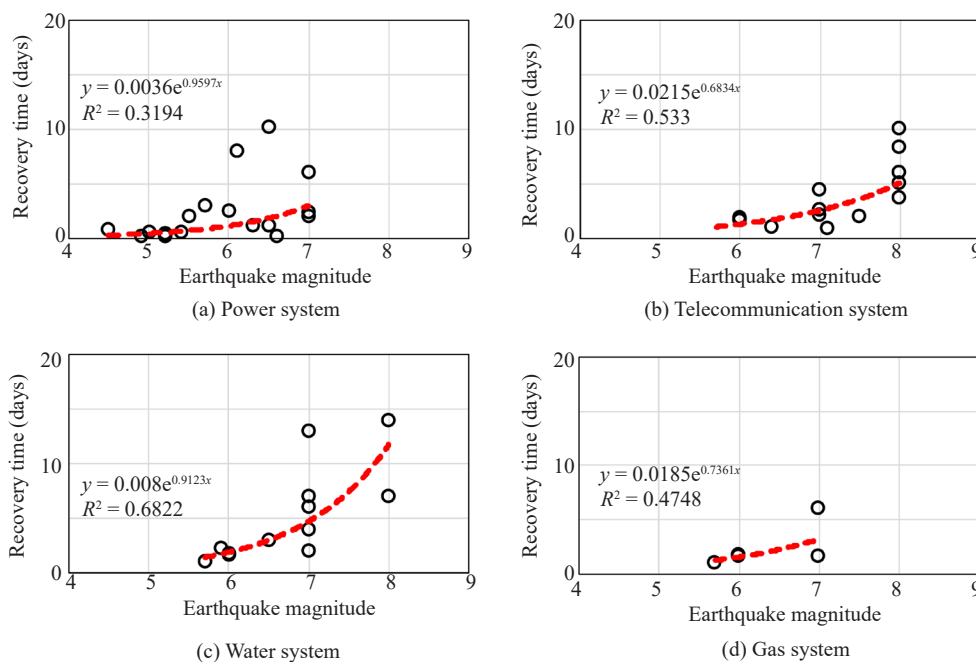

(a) Power system

$$y = 0.0036e^{0.9597x}$$
$$R^2 = 0.3194$$

(b) Telecommunication system

$$y = 0.0215e^{0.6834x}$$
$$R^2 = 0.533$$

(c) Water system

$$y = 0.008e^{0.9123x}$$
$$R^2 = 0.6822$$

(d) Gas system

$$y = 0.0185e^{0.7361x}$$
$$R^2 = 0.4748$$

Fig. 10　Recovery time of lifeline systems

(a) 1995 Hanshin earthquake (*EM* = 6.9)

(b) 2004 Mid-Niigata earthquake (*EM* = 6.6)

(c) 2011 Christchurch earthquake (*EM* = 6.2)
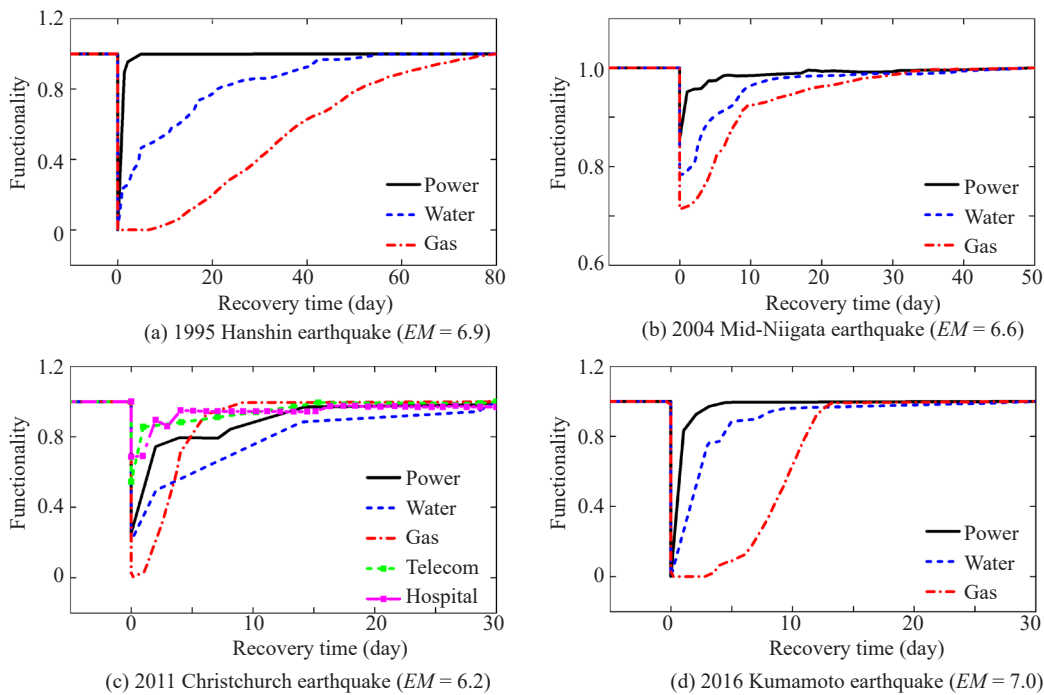
(d) 2016 Kumamoto earthquake (*EM* = 7.0)

Fig. 11   Resilience curves of lifeline systems in recent earthquakes (Monsalve and Llera, 2019)

differences in the political system and policies between China and other countries.

5 A case study: demand and capacity analysis of medical facilities

To demonstrate the completeness of the data included in the benchmark city, a simple case study was conducted, which analyzed the variations of demand and capacity of the medical emergency system of the benchmark city. Two indicators were employed to quantify the functionality of the medical emergency system: the accessibility of hospitals, and the number of available beds and medical staff in the hospitals.

5.1 Service area and accessibility of hospitals

According to the planning and the administrative districts, the service areas of eight hospitals are shown in Fig. 12, where the number of settlements covered by the nearest hospital is listed in the bracket. All settlements can be covered by the eight hospitals. Before an earthquake happens, an area with less than 4 minutes travel time from the closest hospital to a residential unit covers 84.3% of the residential area, while the rest, about 15.7%, can be accessed within 8 min. Travel time is calculated by the length of the shortest route divided by the average speed, which is determined by the type of road and the statistical passage of time.

Calculation of travel time after earthquakes is based on road width considering building collapse, seismic damage of roads, and the effects on travel speed (Xu,
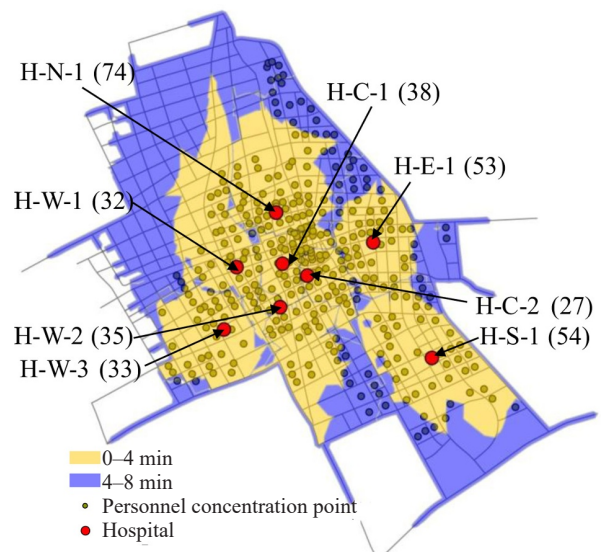

Fig. 12 Service area and accessible time before earthquake

2019). Using the fragility models included in the database and debris falling models from Xu (2019), the numbers of impassable roads, affected roads, and untouched roads after a maximum considered earthquake of intensity VIII are 32, 205, and 896, respectively. The travel time after the earthquake is shown in Fig. 13(a), and compared with that before the earthquake in Fig. 13(b). There are 32 roads that are impassable, most distributed in the downtown area.

The accessibility from residential units to the closest hospital after the earthquake is shown in Fig. 14(a).

The areas accessible in 4 minutes cover 71.3% of the residential area, while those accessible in 8 minutes cover 15.2% of the residential area. 12 settlements (as shown in Fig. 14 (b)) are inaccessible as a result of road damage or building damage. It is worth noting that all these inaccessible areas are concentrated in the central old downtown, which are supposed to be the weak point during an earthquake.

5.2 Demand and capacity of hospitals

Using the injury consequence models in buildings, the number of citizens injured during the earthquake is calculated as 2927, about 4.3‰ of the city population, and the distribution is shown in Fig. 15. Eighty-eight residential units do not need medical treatment and most of them are in the west, north of the city. The old masonry residential buildings hurt more people than buildings with better seismic behavior.

Available medical staff and patient beds after an earthquake are the key parameters defining the capacity of a hospital for emergency rescue. Given the building types, fragility models of buildings, and devices, the number of available medical staff and patient beds are calculated and shown as capacity in Fig. 16(a). The demand of medical staff and patient beds are calculated by empirical formulas as shown in Eqs. (2-1) and (2-2) (Nie *et al.*, 2001). It shall be noted that medical staff are sufficient while patient beds are in significant shortage. Among the eight hospitals, only H-C-2 has enough patient beds, as shown in Fig. 16(b).
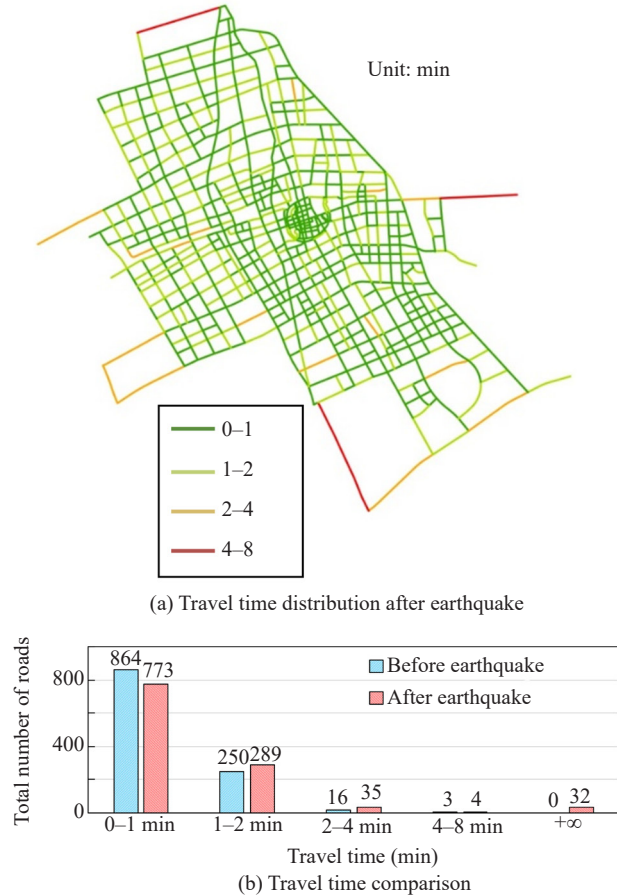
$$D_{MS} = 0.1039\omega \cdot N \qquad (2\text{-}1)$$

$$D_{PB} = 0.2163\omega \cdot N \qquad (2\text{-}2)$$

where N is the number of injured citizens, ω is zone coefficient of the city, D_{MS} is demand of medical staff and D_{PB} is demand of patient beds.
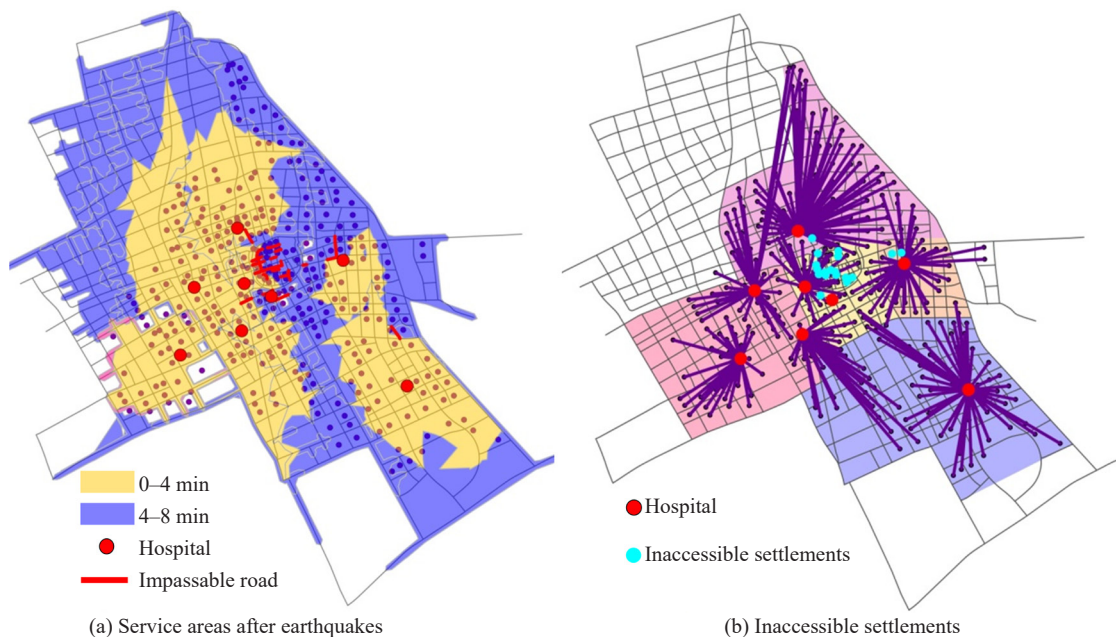

(a) Travel time distribution after earthquake

(b) Travel time comparison

Fig. 13 Travel time after earthquake

(a) Service areas after earthquakes

(b) Inaccessible settlements

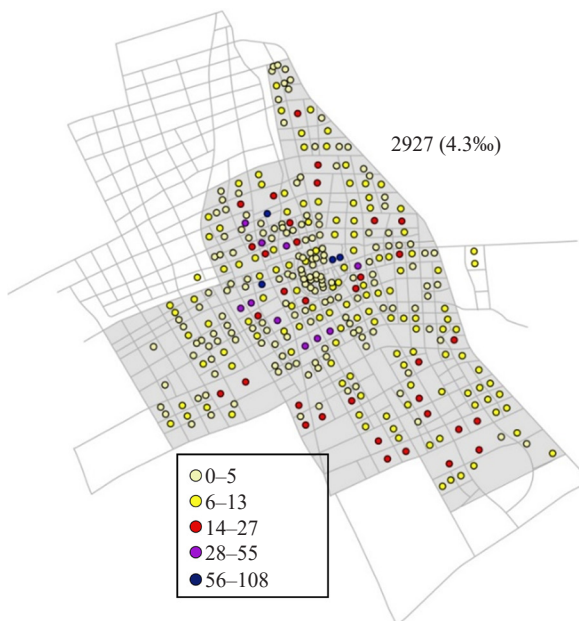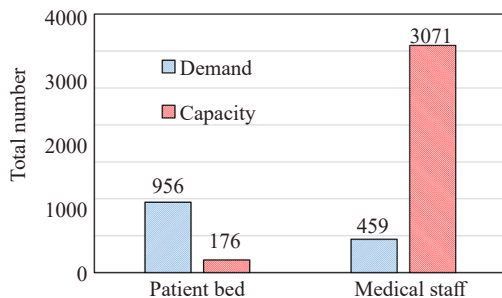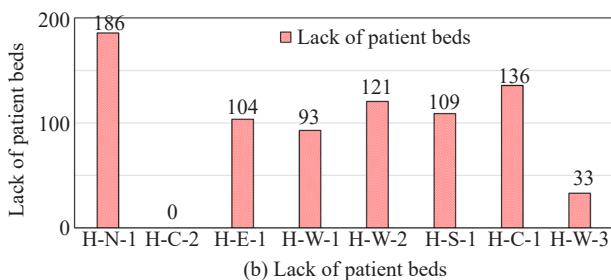**Fig. 14 Hospital capacity after earthquakes**

Fig. 15 Number of people injured during earthquake

(a) Demand and capacity of medical staff and patient beds after earthquakes

(b) Lack of patient beds

Fig. 16 Demand and capacity of medical staff and patient beds after earthquakes

6 Summary

It is well-known that seismic resilience evaluations of cities require interdisciplinary expertise and numerous data models. Current evaluation results of different frameworks or methods have to be calibrated based on a unified evaluation model. To promote the seismic resilience assessment and calibration of different frameworks at a city level, this paper presents a novel benchmark model of a medium-sized city located in the southeastern coastal region of China. The developed model can serve as a testbed to facilitate the construction of a seismic resilient city in China. Similar testbeds of American and European cities such as Centerville virtual community (CVC), Memphis testbed (MTB), and the virtual city of Turin, Italy (VC-TI) are available now. However, Chinese cities are quite different from American and European cities and such a testbed is urgently needed.

Detailed information on the benchmark city, including demographics, site conditions, potential hazard exposure, and building inventory is provided. Descriptions of lifeline systems, including power, transportation, water, drainage, and natural gas distribution networks, as well as hospitals, emergency shelters, and schools designed based on Chinese codes, are also provided. The basic models, including the seismic fragility models, consequence models, and recovery models, are developed based on post-earthquake data obtained from the literature. These models are suitable for seismic resilience assessment and calibration. With these data and models, the seismic performance of the city can be quantified by available assessment frameworks. A preliminary case study on the demand and capacity analysis of medical facilities demonstrated the completeness of the data inventory and model database.

As the first stage of the development of the benchmark city, this study has some limitations, and several extensions need to be explored in future studies. Firstly, the recovery models developed based on limited data need to be updated by collecting more related data. Secondly, analyses of different systems still need to be conducted to comprehensively demonstrate the data completeness. Thirdly, how to quantify the interdependency between different infrastructures and the associated uncertainties still needs more effort.

Acknowledgement

References

Almufti I and Willford M (2013), *REDi™ Rating System: Resilience-Based Earthquake Design Initiative for the Next Generation of Buildings*, San Francisco, CA: Arup.

Bruneau M, Chang SE, Eguchi RT, Lee GC, O'Rourke TD, Reinhorn AM, Shinozuka M, Tierney K, Wallace WA and Winterfeldt DV (2003), "A Framework to Quantitatively Assess and Enhance the Seismic Resilience of Communities," *Earthquake Spectra*, **19**(4): 733–752.

Bruneau M and Reinhorn AM (2007), "Exploring the

Concept of Seismic Resilience for Acute Care Facilities," *Earthquake Spectra*, **23**(1): 41–62.

Burton HV, Deierlein G, Lallemant D and Singh Y (2017), "Measuring the Impact of Enhanced Building Performance on the Seismic Resilience of a Residential Community," *Earthquake Spectra*, **33**(4): 1347–1367.

Chang SE and Shinozuka M (2004), "Measuring Improvements in the Disaster Resilience of Communities," *Earthquake Spectra*, **20**(3): 739–755.

Cimellaro G P, Fumo C, Reinhorn A M and Bruneau M (2009), "Quantification of Disaster Resilience of Health Care Facilities," *Technical Report*, *MCEER-09-0009*, September 14.

Cimellaro GP, Reinhorn AM and Bruneau M (2010), "Seismic Resilience of a Hospital System," *Structure & Infrastructure Engineering*, **6**(1-2): 127–144.

Cimellaro GP, Reinhorn AM and Bruneau M (2011), "Performance-Based Metamodel for Healthcare Facilities," *Earthquake Engineering & Structural Dynamics*, **40**(11): 1197–1217.

Cimellaro GP, Renschler C, Reinhorn AM and Arendt L (2016), "PEOPLES: A Framework for Evaluating Resilience," *Journal of Structural Engineering*, **142**(10): 04016063.

Djalante R, Thomalla F, Sinapoy MS and Carnegie M (2012), "Building Resilience to Natural Hazards in Indonesia: Progress and Challenges in Implementing the Hyogo Framework for Action," *Natural Hazards*, **62**(3): 779–803.

Dong Y and Frangopol DM (2016), "Probabilistic Assessment of an Interdependent Healthcare-Bridge Network System Under Seismic Hazard," *Structure and Infrastructure Engineering*, **13**(1): 160–170.

Ellingwood BR, Cutler H, Gardoni P, Peacock WG, Van d LJW and Wang NY (2016), "The Centerville Virtual Community: a Fully Integrated Decision Model of Interacting Physical and Social Infrastructure Systems," *Sustainable & Resilient Infrastructure*, **1**(3-4): 95–107.

FEMA P58 (2012), *Seismic Performance Assessment of Buildings, Volume 1 Methodology*, Applied Technology Council (ATC), Redwood City, USA.

FEMA (2020), *Summary of Stakeholder Feedback: Building Resilient Infrastructure and Communities (BRIC)*, Federal Emergency Management Agency, Washington, D.C, USA.

Filiatrault A and Sullivan T (2014), "Performance-Based Seismic Design of Nonstructural Building Components: The Next Frontier of Earthquake Engineering," *Earthquake Engineering and Engineering Vibration*, **13**(1): 17–46.

GBJ 11-89 (1989), *Code for Seismic Design of Buildings*, China Architecture and Building Press, Beijing, China. (in Chinese)

GB 50011-2001 (2001), *Code for Seismic Design of Buildings*, China Architecture and Building Press,

Beijing, China. (in Chinese)

GB 50011-2010 (2010), *Code for Seismic Design of Buildings*, China Architecture and Building Press, Beijing, China. (in Chinese)

GB 18306-2015 (2015), *Seismic Ground Motion Parameters Zonation Map of China*, Standardization Administration of China, Beijing, China. (in Chinese)

GB/T 18208.4-2011 (2012), *Post-Earthquake Field Works — Part 4: Assessment of Direct Loss*, Standardization Administration of China, Beijing, China. (in Chinese)

GB/T 38591-2020 (2020), *Standard for Seismic Resilience Assessment of Buildings*, Standardization Administration of China, Beijing, China. (in Chinese)

HAZUS-MH MR3 (2003), "Multi-Hazard Loss Estimation Methodology-Earthquake Model," *Technical Manual*, Department of Homeland Security, Washington, DC, USA.

Hingorania R, Tannera P, Prietob M and Laraa C (2020), "Consequence Classes and Associated Models for Predicting Loss of Life in Collapse of Building Structures," *Structural Safety*, **85**: 101910.

Hong HP and Chao F (2019), "On the Ground-Motion Models for Chinese Seismic Hazard Mapping," *Bulletin of the Seismological Society of America*, **109**(5): 2106–2124.

Hu Y, Dargush GF and Shao XY (2012), "A Conceptual Evolutionary Aseismic Decision Support Framework for Hospitals," *Earthquake Engineering and Engineering Vibration*, **11**(4): 499–512.

Kammouh O, Cimellaro GP and Mahin SA (2018), "Downtime Estimation and Analysis of Lifelines After an Earthquake," *Engineering Structures*, **173**: 393–403.

Kelman I and Glantz MH (2015), "Analyzing the Sendai Framework for Disaster Risk Reduction," *International Journal of Disaster Risk Science*, **6**(2): 105.

Kyriazis P (2013), "Systemic Seismic Vulnerability and Risk Analysis for Buildings, Lifeline Networks and Infrastructures Safety Gain," *SYNER-G FINAL REPORT*, CP-IP 244061, Aristotle University of Thessaloniki, Greece.

Li JC, Wang T and Shang QX (2019), "Probability-Based Seismic Reliability Assessment Method for Substation Systems," *Earthquake Engineering and Structural Dynamics*, **48**: 328–346.

Li YM, Li YZ and Yang BY (2017), "Performance-Based Seismic Fragility Analysis of Steel Frame Structures," *Earthquake Resistant Engineering and Retrofitting*, **39**(4): 55–59. (in Chinese)

Lin QL, Lin JQ and Liu JL (2017), "A Study on the Fragility of Highway Bridges in the Wenchuan Earthquake," *Journal of Vibration and Shock*, **36**(4): 110–118. (in Chinese)

Lu Y, Mosqueda G, Han Q and Zhao Y (2018), "Shaking Table Tests Examining Seismic Response of Suspended

Ceilings Attached to Large-Span Spatial Structures," *Journal of Structural Engineering*, **144**(9): 04018152.

Miles SB and Chang SE (2006), "Modeling Community Recovery from Earthquakes," *Earthquake Spectra*, **22**(2): 439–458.

Monsalve M and de la Llera J C (2019), "Data-Driven Estimation of Interdependencies and Restoration of Infrastructure Systems," *Reliability Engineering & System Safety*, **181**: 167–180.

National Institute of Standards and Technology (NIST) (2016), "Community Resilience Planning Guide for Buildings and Infrastructure Systems," *NIST Special Publication 1190*, U.S. Department of Commerce.

Nie GZ, Gao JG, Su GW and Wang JM (2001), "Models on Rapid Judgement for the Emergent Rescue Needs During Earthquake," **23**(1): 69–76. (in Chinese)

Noori AZ, Marasco S, Kammouh O, Domaneschi M and Cimellaro GP (2017), "Smart Cities to Improve Resilience of Communities," *8th International Conference on Structural Health Monitoring of Intelligent Infrastructure*, Brisbane, Australia, December 5-8.

Pali T, Macillo V, Terracciano M T, Bucciero B, Fiorino L and Landolfo R (2018), "In-Plane Quasi-Static Cyclic Tests of Nonstructural Lightweight Steel Drywall Partitions for Seismic Performance Evaluation," *Earthquake Engineering & Structural Dynamics*, **47**(6): 1566–1588.

Planning Administration of Rugao (PAR) (2017), "General Urban Planning of Rugao (2013-2030)," Planning Administration of Rugao. (in Chinese)

Pitilakis K, Franchin P, Khazai B and Wenzel H (2014), *SYNER-G: Systemic Seismic Vulnerability and Risk Assessment of Complex Urban, Utility, Lifeline Systems and Critical Facilities: Methodology and Applications*, vol 31. Springer, Netherlands.

Reiner M and McElvaney L (2017), "Foundational Infrastructure Framework for City Resilience," *Sustainable and Resilient Infrastructure*, **2**(1): 1–7.

San Francisco Bay Area Planning and Urban Research Association (SPUR) (2008), "The Resilient City: Defining what San Francisco Needs from Its Seismic Mitigation Policies," *SPUR Report*, SPUR Board of Directors.

Shang QX, Wang T and Li JC (2020), "Seismic Resilience Assessment of Emergency Departments Based on the State Tree Method," *Structural Safety*, **85**: 101944.

Steelman JS and Hajjar JF (2008), "Capstone Scenario Applications of Consequence-Based Risk Management for the Memphis Testbed," Mid-American Earthquake Center, Department of Civil and Environmental Engineering, University of Illinois at Urbana-Champaign, Urbana, Illinois, USA, September.

Taghavi S and Miranda E (2003), "Response Assessment of Nonstructural Building Elements," *PEER Report 2003/05*, Pacific Earthquake Engineering Research Center, Berkeley, CA, USA.

United Nations International Strategy for Disaster Reduction (UNISDR) (2007), *Words into Action: a Guidance for Implementing the Hyogo Framework-Hyogo Framework for Action 2005-2015: Building the Resilience of Nations and Communities to Disasters*, UNISDR, Geneva Switzerland.

United Nations International Strategy for Disaster Reduction (UNISDR) (2015), *Sendai Framework for Disaster Risk Reduction 2015 - 2030*, UNISDR, Geneva Switzerland.

Wang T, Shang QX, Chen X and Li JC (2019), "Experiments and Fragility Analyses of Piping Systems Connected by Grooved Fit Joints With Large Deformability," *Frontiers in Built Environment*, **5**: 49.

Xiong LH (2004), "Study on Seismic Performance of Small Hollow Concrete Block Buildings,"*PhD Dissertation*, Institute of Engineering Mechanics, China Earthquake Administration. (in Chinese)

Xiong C, Huang J and Lu XZ (2020), "Framework for City-Scale Building Seismic Resilience Simulation and Repair Scheduling with Labor Constraints Driven by Time-History Analysis," *Computer-Aided Civil and Infrastructure Engineering*, **35**(4): 322–341.

Xu MY (2019), "Seismic Fragility Analysis of Frame-Shear Structures Based on New Intensity Measures and CPU Parallel Computing," *Master Dissertation*, Harbin Institute of Technology. (in Chinese)

Yodo N and Wang P (2016), "Engineering Resilience Quantification and System Design Implications: A Literature Survey," *Journal of Mechanical Design*, **138**(11): 111408.

Yu XH, Lu D and Li B (2016), "Estimating Uncertainty in Limit State Capacities for Reinforced Concrete Frame Structures Through Pushover Analysis," *Earthquakes and Structures*, **10**(1): 141–161.